IARJSET

ISSN (Online) 2393-8021
ISSN (Print) 2394-1588

International Advanced Research Journal in Science, Engineering and Technology

Vol. 8, Issue 3, March 2021

DOI: 10.17148/IARJSET.2021.8301

Experimental Research of a Diesel Engine with Electronic Control

Leonard-Iulian Cucu [1], Ion Copae [2]

Eng., S.A-R City Insurance, Bucharest, Romania[1]

Professor Eng., Department of Military Vehicles and Transportation, Military Technical Academy "Ferdinand I", Bucharest, Romania[2]

Abstract: The paper presents some experimental results related to the operation of an electronically controlled diesel engine that equips a car. The most frequent dynamic regimes during the car tests are highlighted. The statistical analysis of the experimental data is presented. Some dependencies between the quantities related to the operation of the engine in dynamic regime are given and mathematical models are established.

Keywords: Diesel engine, common-rail, electronic control, engine load and engine speed.

I. INTRODUCTION

The paper focuses on one of the most widely used engines in automobiles today [1, 7]. This is the compression ignition engine (Diesel engine), the most controversial energy source on vehicles in recent times, especially after the Volkswagen dispute, which highlighted major deviations from anti-pollution rules during the operation of vehicles. However, Diesel engines currently manufactured meet the requirements of anti-pollution regulations, even if they have become more complex and more expensive. The engines manufactured today have an electronic operation management by being equipped with sensors, actuators and microcontrollers, all of which ensure real-time operation control. In this way, the current diesel engine has become more efficient, more powerful, quieter, more economical and cleaner. A current diesel engine has different electronic control systems, the main ones being: fuel injection control system, supercharged air pressure control system, recirculated gas quantity control system, pollutant control system, fuel control system start-up, air-fuel mixture quality control system, speed control system etc. [2, 8].

II. EXPERIMENTAL RESEARCH

The experiments were carried out with a Ford Focus car equipped with a turbocharged diesel engine, a common-rail fuel supply system and a recirculated gas control system. The acquisition of the functional parameters was made using Ford's FoCOM interface and software. From the data obtained, 100 more significant experimental tests were selected for the purposes pursued (marked F1-F100), which mark the frequent load and speed regimes during operation.

Thus, in fig.1 are presented the instantaneous values of the engine torque M_e and of the engine power P_e, in the graphs being also represented the minimum, average and maximum values of the quantities. The maximum values of torque (215 Nm) and power (66 kW) in the technical specifications of the engine are also highlighted.

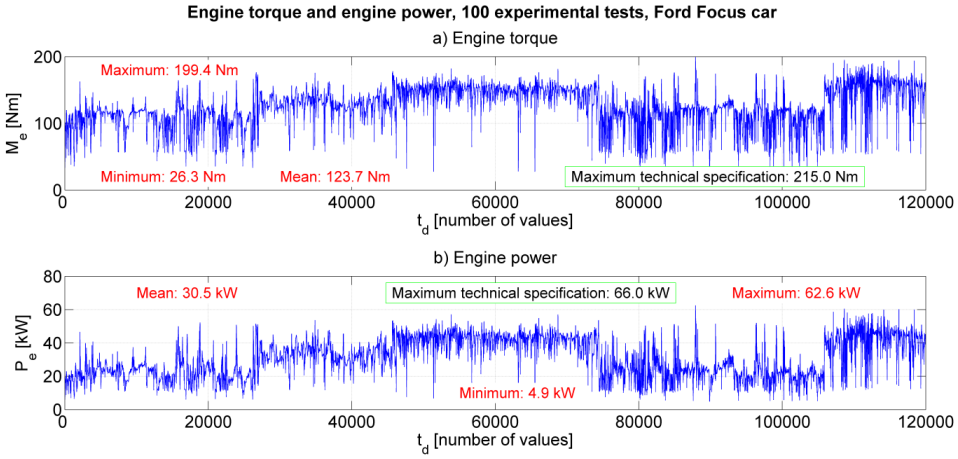

Fig. 1 Engine torque and engine power of the Ford Focus car

IARJSET

ISSN (Online) 2393-8021
ISSN (Print) 2394-1588

International Advanced Research Journal in Science, Engineering and Technology

Vol. 8, Issue 3, March 2021

DOI: 10.17148/IARJSET.2021.8301

From fig.1a it results that during the experiments, the engine torque varied in the interval 26.3-199.4 Nm, the average on all the tests being of 123.7 Nm.

Fig. 1b shows that the engine power varied in the range of 4.9-62.6 kW, the average of all tests being 30.5 kW.

Fig. 2 shows the values of load and engine speed n, first by the air pressure allowed in the cylinders p_a. As can be seen from Fig. 2a, all values of the pressure p_a are higher than 100 kPa, which confirms that the engine is supercharged.

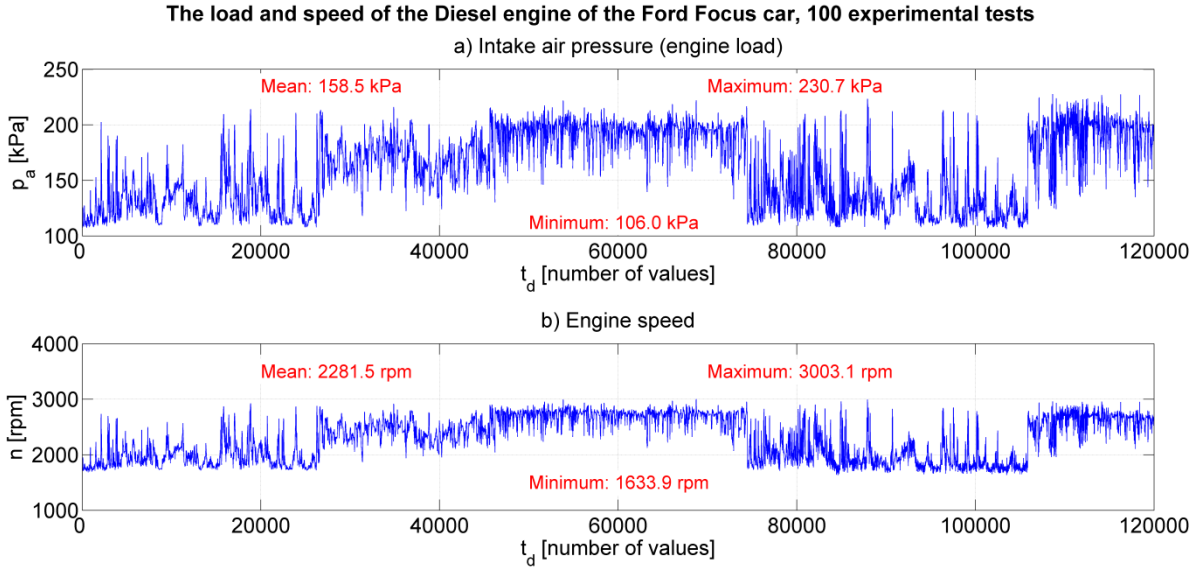

Fig. 2 Air pressure in the intake manifold (engine load) and engine speed

Fig. 3 shows the hourly fuel consumption C_h and the cyclic fuel flow c_c. The cyclic fuel flow is calculated with formula:

$$c_c = \frac{100 C_h}{3nz} \tag{1}$$

where: C_h [kg/h] - hourly fuel consumption of the engine, established experimentally; n [rpm] - engine speed, established experimentally; z - number of engine cylinders.

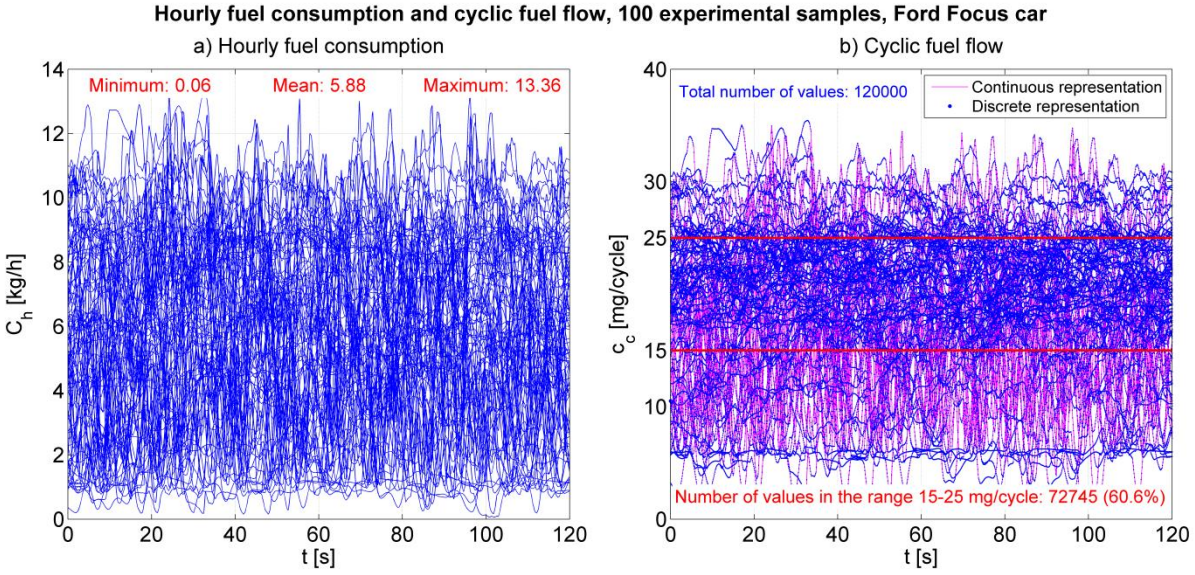

Fig. 3 Hourly fuel consumption and cyclic fuel flow

IARJSET

ISSN (Online) 2393-8021
ISSN (Print) 2394-1588

International Advanced Research Journal in Science, Engineering and Technology

Vol. 8, Issue 3, March 2021

DOI: 10.17148/IARJSET.2021.8301

In fig.1 and fig.2 the 100 experimental tests are arranged one after the other, and in fig.3 they are superimposed; as a result in the first case (fig.1 and fig.2) on the abscissa axis is the discrete time t_d [number of values], and in the second case (fig.3) is the continuous time t [s]. In fig.3b there is a continuous representation and a discrete representation of the data, the last being the real one (the experimental data having a discrete character).
The discrete representation in fig.3b allows it to be found more easily that in the interval 15-25 mg/cycle there are 60.6% (72745 values) of the total number of values (120000 values).

III. STATISTICAL DATA ANALYSIS

Based on the experimental data and using the corresponding calculation relations, the usual first order statistical characteristics used can be obtained: mean, variance, standard deviation, minimum value, maximum value, norm 1, norm 2, infinite norm, etc. Because the experimental data constitute discrete finite series, the computational relations are those related to this character [3, 4, 5].

Thus, the mean value m_x, the standard deviation σ_x and the variance D_x are calculated with the expressions, for a finite number of n data of any size x:

$$m_x = \frac{1}{n}\sum_{i=1}^{n} x_i \; ; \; \sigma_x = \sqrt{\frac{1}{n}\sum_{i=1}^{n}\left(x_i - m_x\right)^2} \; ; \; D_x = \frac{1}{n}\sum_{i=1}^{n}\left(x_i - m_x\right)^2 \tag{2}$$

The norm 1 or the sum of the absolute values (denoted L_1), the norm 2 or the Euclidean norm (denoted L_2) and the infinite norm or the supreme value (denoted L_∞) are established with the relations:

$$\|x\|_1 = L_1 = \sum_{i=1}^{n}|x_i| \; ; \; \|x\|_2 = L_2 = \sqrt{\sum_{i=1}^{n}|x_i|^2} \; ; \; \|x\|_\infty = L_\infty = \sup_i |x_i| \tag{3}$$

Another quantity used is the Coefficient Of Variation (COV), which, for a given quantity x, is given by the ratio between the standard deviation σ_x and the mean value m_x:

$$\mathrm{COV}_x = \frac{\sigma_x}{m_x} \tag{4}$$

Thus, in fig.4a the main statistical quantities for the hourly fuel consumption are shown, and in fig.4b for the engine torque, both at test F92. It is found that at both parameters, the maximum value is the same as the infinite norm.

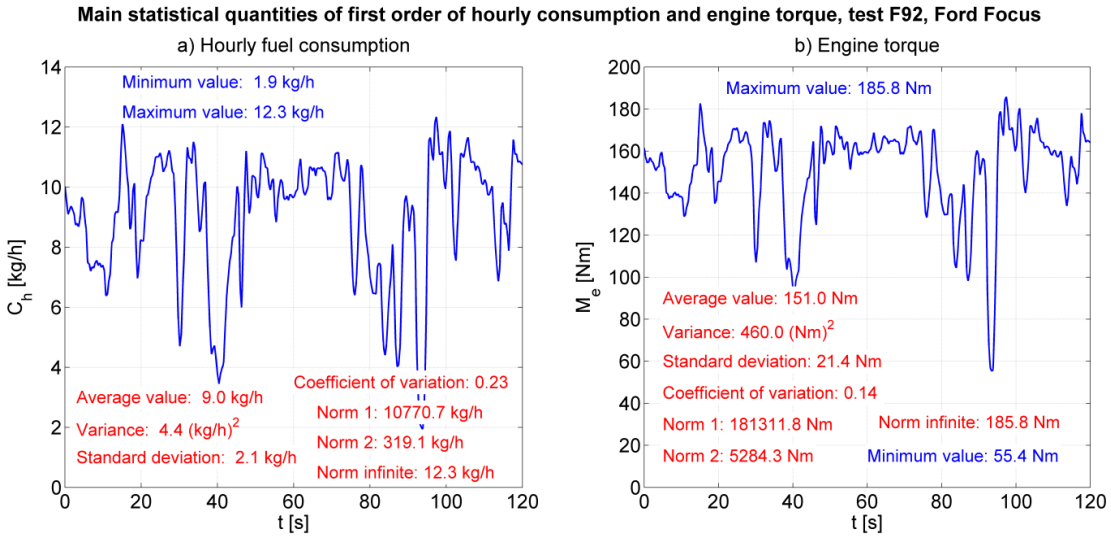

Fig. 4 First-order statistical characteristics of hourly fuel consumption and engine torque

IARJSET

ISSN (Online) 2393-8021
ISSN (Print) 2394-1588

International Advanced Research Journal in Science, Engineering and Technology

Vol. 8, Issue 3, March 2021

DOI: 10.17148/IARJSET.2021.8301

The graphs in fig.5 show the average values on tests of the engine torque M_e and of the engine power P_e. From fig.5a it results that the average values on tests of the engine torque vary in the range 88.6-156.3 Nm, with an average on the set of tests of 123.7 Nm. Fig. 5b shows that the average values per tests of engine power vary in the range 17.3-44.1 kW, with an average of all tests of 30.5 kW.

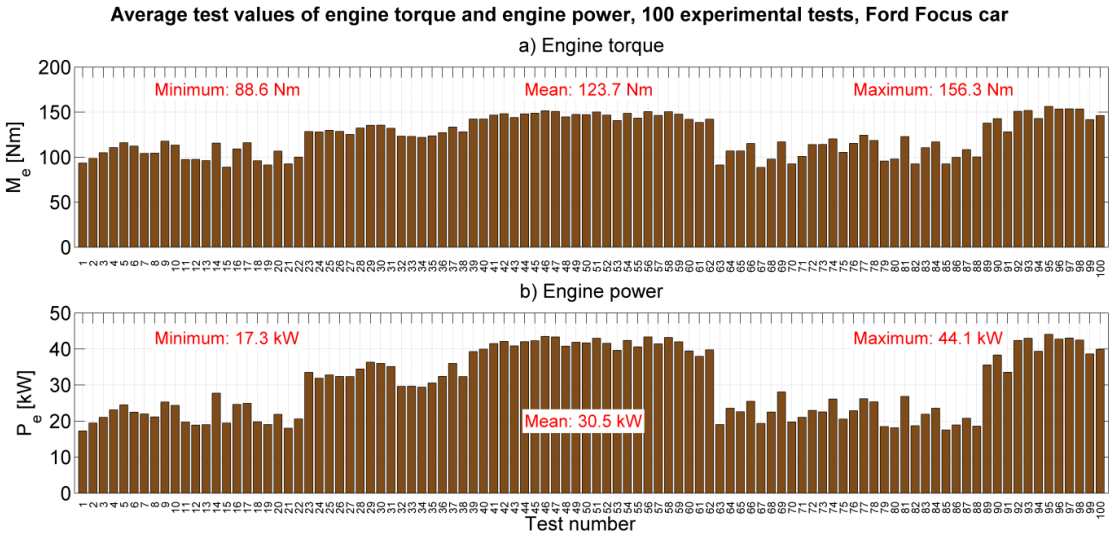

Fig. 5 Mean values on engine torque and engine power tests

The graphs in Fig. 6 show the average values on tests of the effective specific fuel consumption c_e and of the effective engine efficiency η_e, established with the expressions [9, 10]:

$$c_e = 1000\frac{C_h}{P_e};\ \ \eta_e = \frac{36\cdot 10^5}{c_e Q_i} \tag{5}$$

where Q_i represents the lower calorific power of the fuel.

Fig. 6a shows that the average values per test of the effective specific fuel consumption vary in the range 178.6-281.4 g/(kWh), with an average of all tests of 234.5 g/(kWh).

Fig. 6b shows that the average values per test of the effective engine efficiency vary in the range of 23.6-38.2%, with an average of all tests of 31.3%.

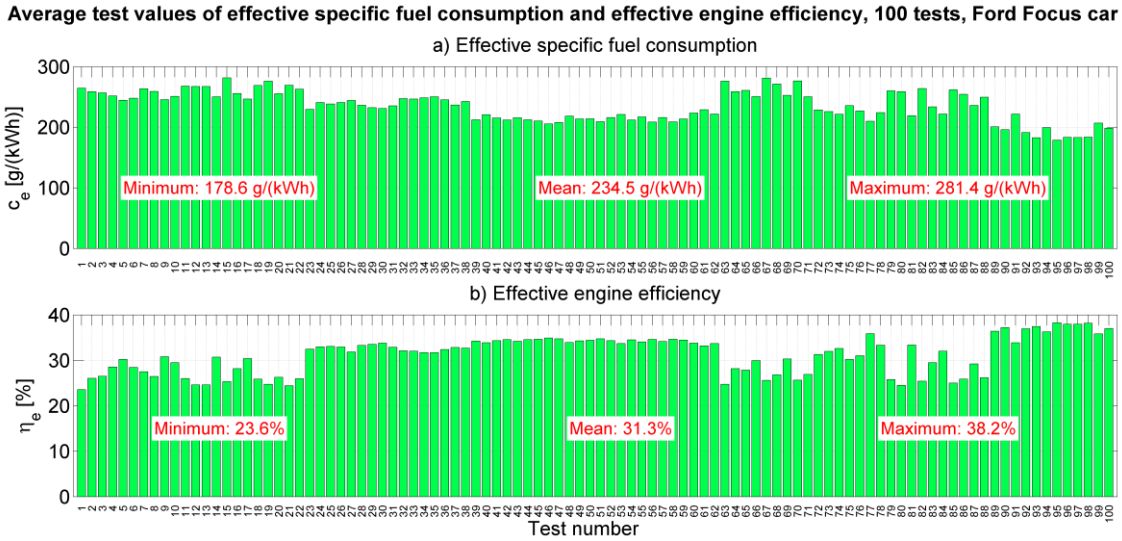

Fig. 6 Average test values of effective specific fuel consumption and effective engine efficiency

IARJSET

ISSN (Online) 2393-8021
ISSN (Print) 2394-1588

International Advanced Research Journal in Science, Engineering and Technology

Vol. 8, Issue 3, March 2021

DOI: 10.17148/IARJSET.2021.8301

Fig. 7 shows the maximum values on tests of the percentage of recirculated gas γ and of the angle of inclination of the turbine blades α. The percentage of recirculated gas is determined by the relation:

$$\gamma = \frac{C_g}{C_a + C_g} \cdot 100\% \tag{6}$$

where C_a represents the hourly air consumption, and C_g the amount of recirculated gases.

From Fig.7a it can be deduced that the maximum values on tests of the percentage of recirculated gases vary in the range of 14.8-29%, with an average of 24.3% on all tests. Fig. 7b shows that the maximum values on the tests of the inclination angle of the turbine blades vary in the range of 21.5-54.2 degrees, with an average of all the tests of 43.9 degrees.

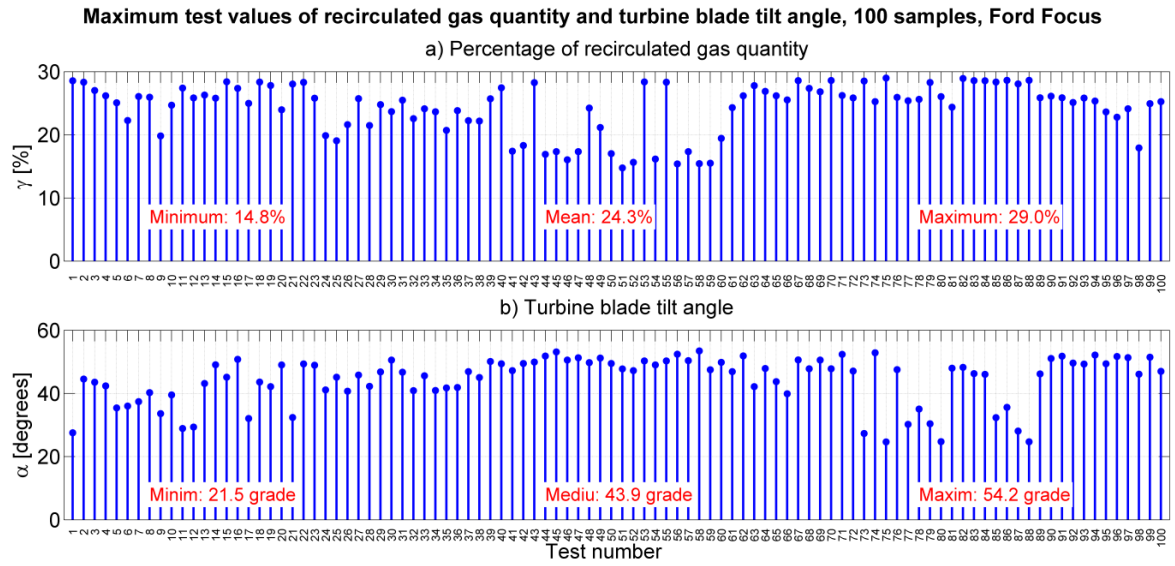

Fig. 7 Maximum values on tests of the amount of recirculated gas and the tilt angle of the turbine blades

Fig. 8 shows the maximum test values of the accelerator pedal position p and engine speed n. Fig. 8a shows that the maximum test values of the accelerator pedal position vary in the range of 55.8-100%, with an average of the total samples of 80.2%.

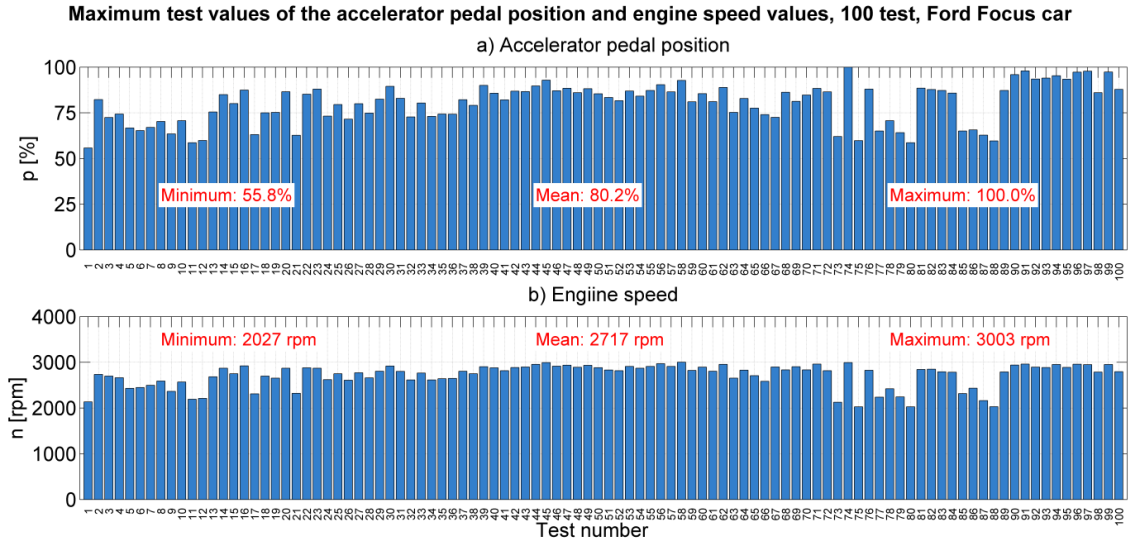

Fig. 8 Maximum values on the tests of the position of the accelerator pedal and the engine speed

IARJSET

ISSN (Online) 2393-8021
ISSN (Print) 2394-1588

International Advanced Research Journal in Science, Engineering and Technology

Vol. 8, Issue 3, March 2021

DOI: 10.17148/IARJSET.2021.8301

Fig. 8b shows that the maximum values on tests of engine speed vary in the range 2027-3003 rpm, with an average of all tests of 2717 rpm.

IV. FUNCTIONAL DEPENDENCIES

The existence of electronic control of the diesel engine has as a consequence the supervision of its operation by the on-board computer and as a result it is expected that the functional dependencies between parameters will be more accentuated than in a classic engine. Functional dependencies can also be highlighted with the help of graphs.

For example, Fig. 9 graphically illustrates the functional dependence between the positions of the accelerator pedal p, the engine torque M_e and the cyclic fuel flow c_c.

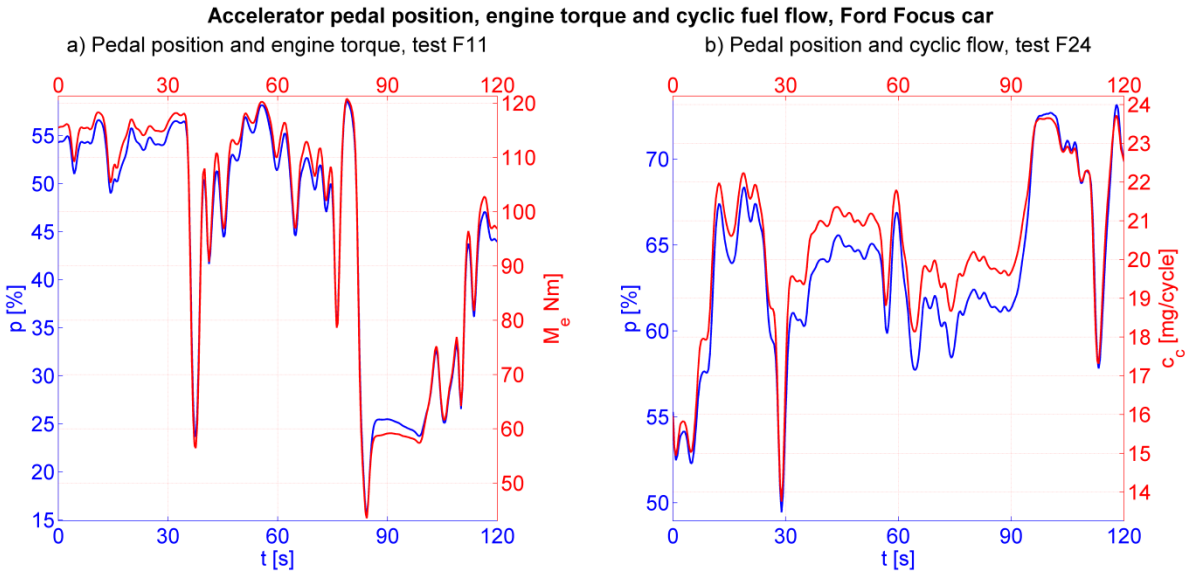

Fig. 9 Dependencies between accelerator pedal position, engine torque and cyclic fuel flow

Similarly, Fig. 10 graphically shows the functional dependence between the position of the accelerator pedal p, the intake air pressure p_a and the hourly air consumption of the engine C_a.

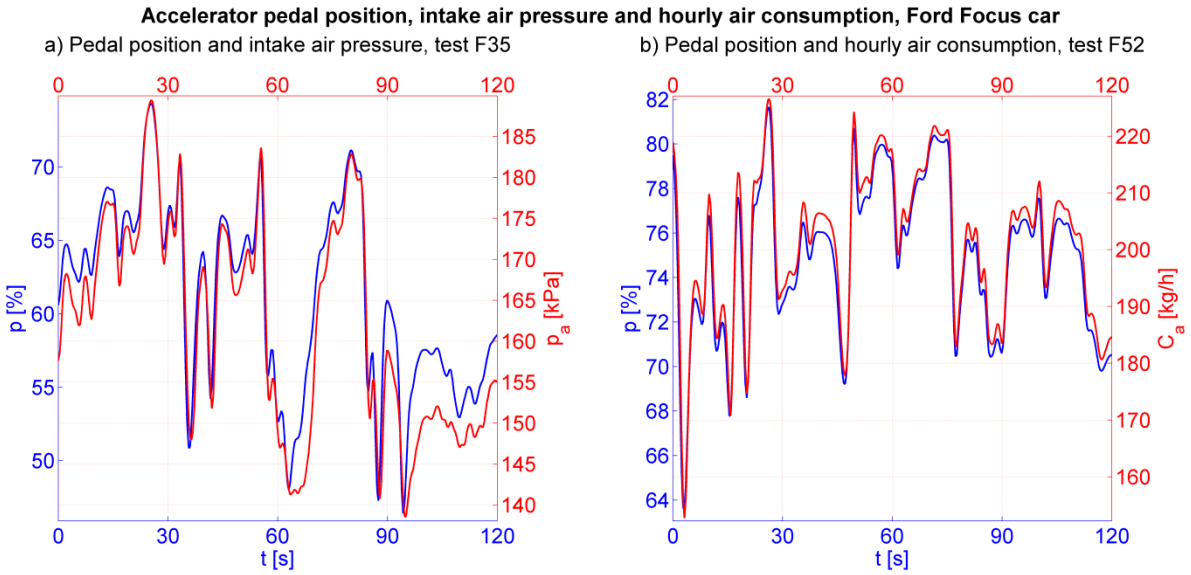

Fig. 10 Dependencies between the accelerator pedal position, intake air pressure and the hourly air consumption

The existence of functional dependencies also allows the deduction of mathematical models of engine operation in dynamic mode and at steady state, in the latter case by establishing static characteristics.

IARJSET

ISSN (Online) 2393-8021
ISSN (Print) 2394-1588

International Advanced Research Journal in Science, Engineering and Technology

Vol. 8, Issue 3, March 2021

DOI: 10.17148/IARJSET.2021.8301

V. MATHEMATICAL MODELS OF ENGINE OPERATION

Based on experimental data, different mathematical models can be established [6]. For example, for the beginning, mathematical models are established that will highlight the dependencies between the parameters through the average values on their tests, sometimes being visualized also the dependencies between the instantaneous values of the quantities. Later, other mathematical models will be established, but using the instantaneous values of the parameters.

Thus, in fig.11a is shown the dependence between the instantaneous values of the hourly air consumption C_a, as well as the intake air pressure p_a, and in fig.11b between the average values on their samples (C_{am} and p_{am}), including the calculation relation (1), both graphs highlighting a direct dependence. Fig. 11b also shows the 98% upper and lower confidence intervals.

Fig. 11b shows the dependence between the average values of the intake air pressure p_{am} and the hourly air consumption C_{am}:

$$C_{am} = 0.00604\,p_{am}^2 - 0.17666\,p_{am} + 9.928 \tag{7}$$

Fig. 12 shows the dependencies between the average values of the engine torque M_{em} and the power P_{em} and the speed n_m, and in fig.13 between the average values of the torque and power depending on the position of the accelerator pedal p_m.

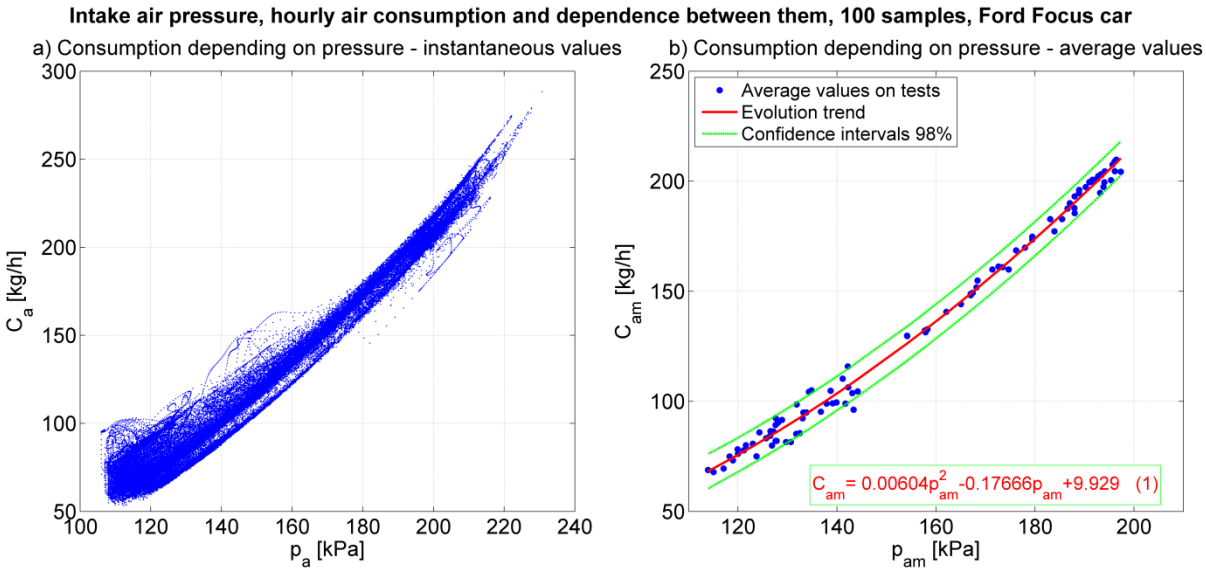

Fig. 11 Mathematical model of form C_{am}=f(p_{am})

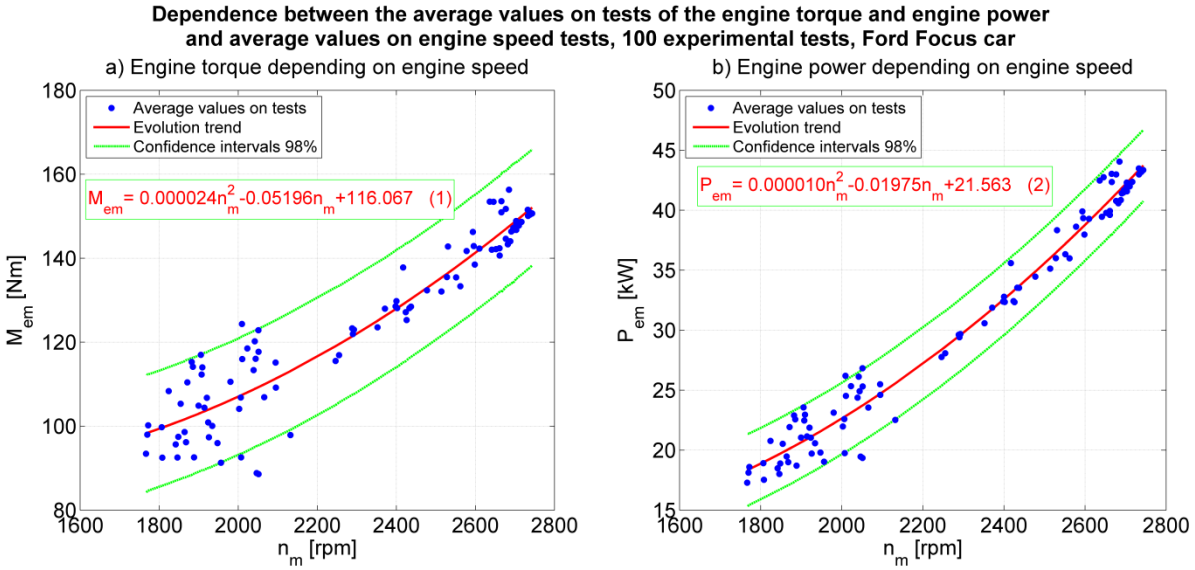

Fig. 12 Mathematical models of form M_{em}=f(n_m) și P_{em}=f(n_m)

IARJSET

ISSN (Online) 2393-8021
ISSN (Print) 2394-1588

International Advanced Research Journal in Science, Engineering and Technology

Vol. 8, Issue 3, March 2021

DOI: 10.17148/IARJSET.2021.8301

For example, Fig. 12a shows the dependence between the average values of the engine speed n_m and the engine torque M_{em}:

$$M_{em} = 0.000024n_m^2 - 0.05196n_m + 116.067 \quad (8)$$

in the presented graphs being rendered also the other analytical expressions of the mathematical models.

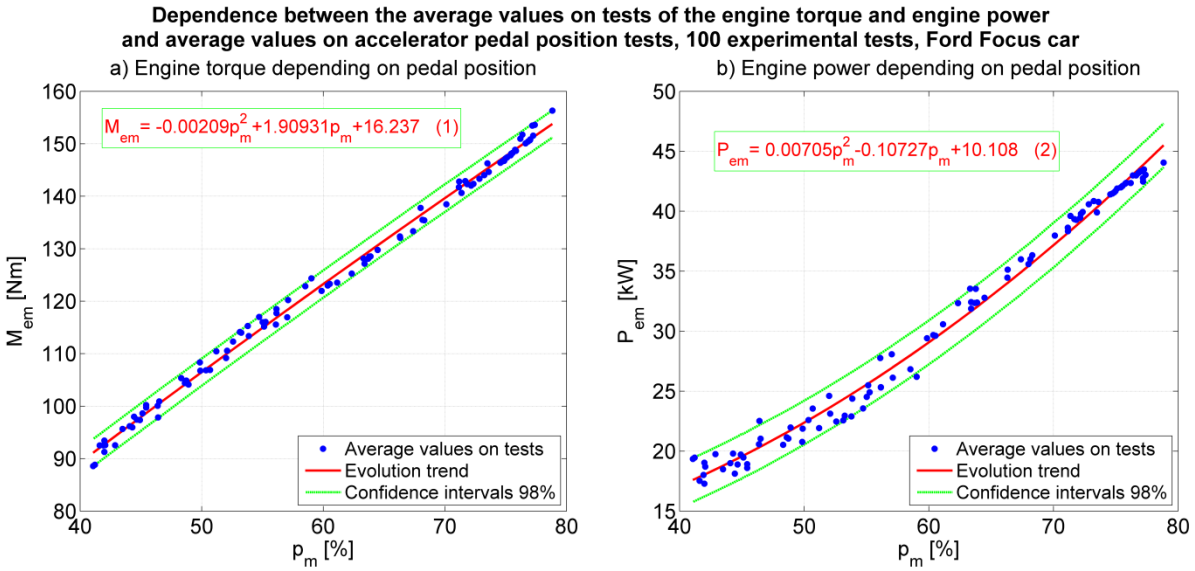

Fig. 13 Mathematical models of form M_{em}=f(p_m) și P_{em}=f(p_m)

Fig. 14 shows the results of establishing a mathematical model that provides the values of the motor torque M_e depending on the speed n and the engine load, the last by the position of the accelerator pedal p, for all 100 experimental tests; this model is the spatial static characteristic M_e = f (n, p) of the engine. The graph shows the area of commutation of the static characteristic with the analytical expression (1), as well as the 120000 experimental values.

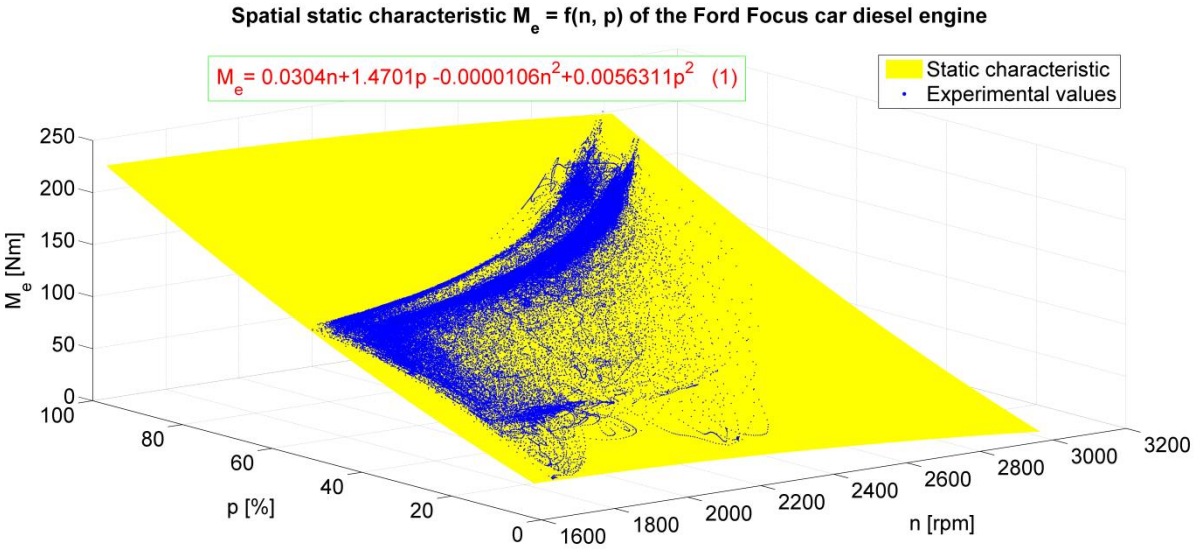

Fig. 14 Mathematical model of form M_e=f(n, p), spatial representation

Fig. 14 shows the analytical expression of the dependence between the instantaneous values of the engine speed, the position of the accelerator pedal and the engine torque, for all 100 experimental tests:

$$M_e = 0.0304n + 1.4701p - 0.0000106n^2 + 0.0056311p^2 \quad (9)$$

IARJSET

ISSN (Online) 2393-8021
ISSN (Print) 2394-1588

International Advanced Research Journal in Science, Engineering and Technology

Vol. 8, Issue 3, March 2021

DOI: 10.17148/IARJSET.2021.8301

similarly other generalized mathematical models can be established.

Fig. 15 shows the same static characteristic of fig. 14, but in contour representation. In this case the rendered curves are of iso-torque (M_e = const.).

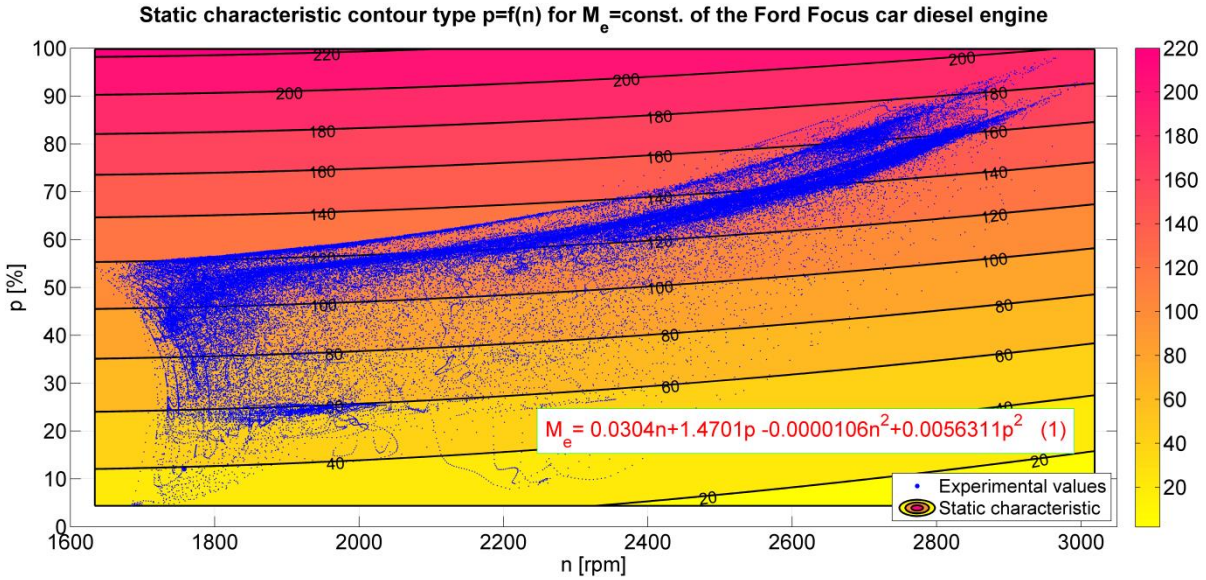

Fig. 15 Mathematical model of form M_e=f(n, p), contour representation

VI. CONCLUSION

Experimental research conducted with an electronically controlled diesel engine benefits from the existence of built-in sensors and actuators, an on-board computer and specialized equipment for data acquisition and storage.

Based on the data purchased from the on-board computer, the operation of the engine at different loads and speeds is analyzed. Experiments have shown that the engine runs predominantly at partial loads and very little at full load.

Also, based on experimental data can be established customized or generalized mathematical models, which can be used to control the engine and to optimize its performance.

REFERENCES

[1]. J. Chauvin ș. a., Modeling and control of a Diesel HCCI engine, Institut Francais du Petrol, 2017, Fifth IFAC Symposium on Advances in Automotive Control, Seascape Resort : United States (2007)". DOI : 10.3182/20070820-3-US-2918.00064

[2]. Li. Cheng, Transient modeling of a Diesel engine and air-path control. Doctoral Thesis, University of Sussex, 2015. http://sro.sussex.ac.uk/id/eprint/55340/

[3]. M. Huang ș.a., Toward Real-Time Automotive Model Predictive Control: A Perspective from a Diesel Air Path Control Development, 2018, DOI: 10.23919/ACC.2018.8431407

[4]. R. Islam, S. Hasan, Integration of Mechanical Systems with IoT, International Advanced Research Journal in Science, Engineering and Technology (IARJSET), Vol. 8, Issue 1, January 2021, pag. 43-50

[5]. A. Mehmood, Modeling, simulation and robust control of an electro-pneumatic actuator for VGT., These de Doctorat, Universite de technologie Belfort-Montbeliard, 2013. https://tel.archives-ouvertes.fr/file/index/docid/827445/

[6]. A. Shamdani ș.a., Air intake modeling with fuzzy AFR control of a turbo- charged Diesel engine, International Journal Vehicle Systems Modelling and Testing, Vol. 3, No. 1/2, 2008, page 114-138. https://doi.org/10.1504/IJVSMT.2008.020621

[7]. J. Singh, A review on system in Diesel engines, International Journal of Advanced Technology in Engineering and Science, vol. 4, mai 2016. https://www.ijates.com/images/short_pdf/1464436108_161ijates.pdf

[8]. X.T. Tran, Modelling and simulation of electronically controlled Diesel injectors, Thesis, 2003, Sydney. https://trove.nla.gov.au/work/3755191.

[9]. R. Vilău, I. Lespezeanu, M. Singureanu, Considerations regarding the influence of inappropriate electronic throttle unit operation on pollutant emissions of internal combustion engines, 5th International Scientific Conference SEA-CONF 2019, IOP Conf. Series: Journal of Physics: Conf. Series 1297 (2019) 012032, IOP Publishing, doi:10.1088/1742-6596/1297/1/012032

[10]. L. Barothi, D. Voicu, R.-M. Stoica, M. Singureanu, Recording of parameters characteristic to engine and vehicle in order to validate a simulation model for fuel consumption, 5th International Scientific Conference SEA-CONF 2019, 17–18 May 2019, Mircea cel Batran Naval Academy, Constanta, Romania, IOP Conf. Series: Journal of Physics: Conf. Series 1297 (2019) 012030 IOP Publishing, doi:10.1088/1742-6596/1297/1/012030